Plasma Actuator Control of a Lifted Ethane Turbulent Jet Diffusion Flame

Seong-kyun Im, Moon Soo Bak, Mark Godfrey Mungal, and Mark A. Cappelli

***Abstract*— A dielectric barrier discharge (DBD) actuator is used to stabilize the base of a lifted ethane turbulent jet diffusion flame by modifying the coflow velocity field. The velocity field and flame base are measured by particle image velocimetry and unfiltered flame chemiluminescence imaging, respectively. An axisymmetric DBD actuator, integrated onto the nozzle body and driven by 8 kHz, 10–12-kV peak-to-peak sinusoidal voltage, generates the directional flow that opposes the coflow that surrounds the jet nozzle. This flow induces a separation bubble that retards and diverts the surrounding fluid further away from the fuel jet. The turbulent jet diffusion flame liftoff height is found to be significantly reduced by this plasma actuation.**

***Index Terms*— Plasma application.**

I. Introduction

THE STABILIZATION of lifted turbulent jet diffusion flames in coflow air with bluff bodies has drawn much attention because of the increased interest in low-emission/high-power combustion of gaseous hydrocarbons. Bluff bodies introduced into the coflow stream generate separation bubbles that reduce the momentum of the coflowing air near the region of the fuel jet exit. As a consequence, this manipulation of the coflow increases the residence time of the fuel/air mixture, enhancing heat transfer from the flame to the unburned gas mixture, thereby allowing otherwise strongly lifted turbulent jet diffusion flames to anchor closer to the fuel jet nozzle [1]–[4]. Although this method induces an additional drag on the flow [5], more importantly, it has a fixed geometry and therefore hinders adaptive flow control. In this paper, we propose and demonstrate the use of surface dielectric barrier discharge (DBD) actuator for controlling the coflow air surrounding turbulent jet diffusion flames, generating flow recirculation through actuator-induced flow separation.

DBD actuator-based flow control has been the subject of research for over two decades [6]. A typical DBD actuator consists of a pair of electrodes separated by a dielectric material, with one of the electrodes exposed to the external flow. These electrode pairs create an atmospheric pressure air discharge usually driven by ac. Positive (N_2^+) and negative (O_2^-) ions [7], [8] generated by the discharge migrate in response to the applied oscillating field, transferring momentum to the background air generating an asymmetric directional force on the flow. The vast majority of applications of these discharges have been in the actuation of boundary layers for control of separation in both subsonic and supersonic flow regimes [9]–[14].

In many DBD flow control applications, the electrode geometries are arranged to induce a force that is either in the streamwise or spanwise direction. The typical actuators induce a wall jet that is on the order of few mm thick with maximum wall jet speeds reaching as high as 10 m/s [6]. When oriented to induce a streamwise force on the flow, this wall jet adds streamwise momentum to the slower speed fluid near the wall enabling the near-wall region to resist adverse pressure gradients that have a tendency to separate the flow [9]–[12]. Although not extensively investigated, electrode pairs oriented to induce a spanwise force also produce directional wall jets. An induced flow in the spanwise direction interacts with the streamwise flow to generate near-wall vortices. Several previous studies showed that the induced vortices can draw higher momentum fluid into the near-wall boundary layer also enabling the flow to resist boundary layer separation [13]–[18]. In this paper, the actuator pair is oriented to produce a wall jet that opposes the incoming coflow air. The flow induced by the DBD actuator in this configuration acts like an imposed pressure gradient in that it generates a separation bubble in its vicinity. As a result of this actuation, when integrated into the body of a jet-diffusion flame nozzle in surrounding coflow air, the surrounding air responds as if there is a bluff body present, diverting air flow and increasing the residence time of the fuel–air mixture. Using this actuation mechanism, we demonstrate the ability of these actuators to stabilize an ethane turbulent jet diffusion flame base.

II. Experimental Setup

A vertically operated wind tunnel having a 50 cm by 50 cm cross sectional test section is used throughout the study. It operates at speeds of 0.3, 0.45, and 0.6 m/s, which are in the range of 0.75 to 1.5 times ethane laminar flame speed (S_L). This tunnel has a honeycomb and metal screen straightener at the upstream of the test section for flow conditioning. The cylindrical ethane jet nozzle body of outer diameter $D_b = 10$ mm is placed at the center of this wind tunnel, as schematically shown in Fig. 1(a). The inner diameter of

Manuscript received April 29, 2013; revised July 2, 2013; accepted August 2, 2013. Date of publication August 21, 2013; date of current version December 9, 2013. This work was supported in part by the National Science Foundation and in part by the Department of Energy through the NSF/DOE Partnership in Basic Plasma Science. The work of M. Bak was supported in part by a Stanford Graduate Fellowship.

S.-K. Im, M. S. Bak, and M. A. Cappelli are with the Department of Mechanical Engineering, Stanford University, Stanford, CA 94305-3030 USA (e-mail: sim3@stanford.edu; moonsoo@stanford.edu; cap@stanford.edu).

M. G. Mungal is with the School of Engineering, Santa Clara University, Santa Clara, CA 95053 USA, and also with the Department of Mechanical Engineering, Stanford University, Stanford, CA 94305-3030 USA (e-mail: mungal@stanford.edu).

Color versions of one or more of the figures in this paper are available online at http://ieeexplore.ieee.org.

Digital Object Identifier 10.1109/TPS.2013.2277722

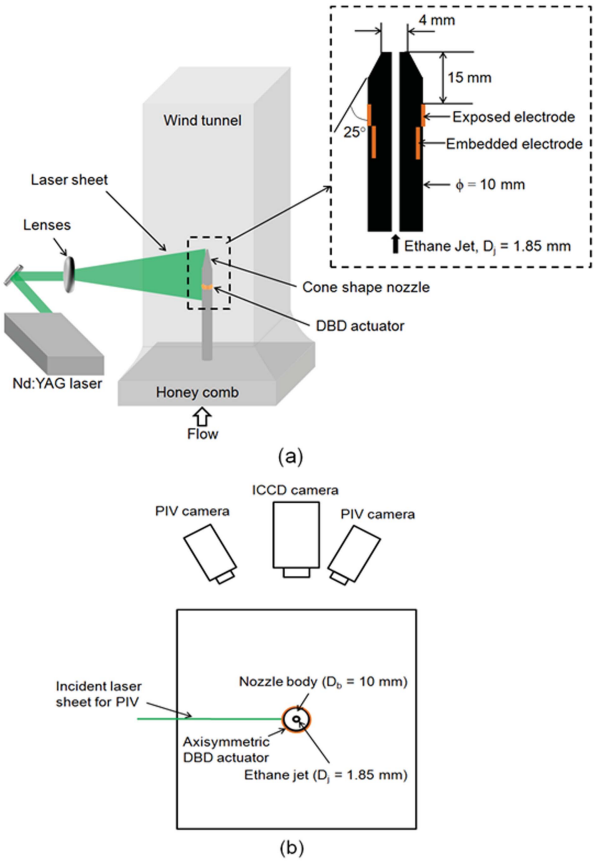

Fig. 1. (a) Overall schematic of the experimental setup and details of jet nozzle geometry. (b) Schematic of cross-sectional view of the test section.

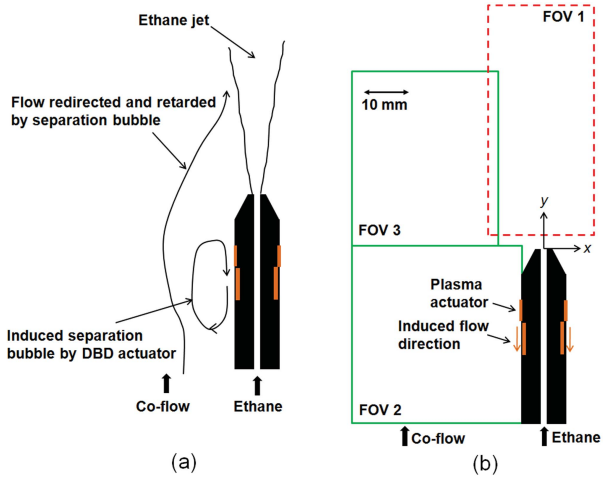

Fig. 2. Schematic of (a) manipulated flow field by the DBD actuator and (b) sPIV and unfiltered flame chemiluminescence imaging FOVs.

the nozzle is $D_j = 1.85$ mm, and is concentric with the nozzle body. In this paper, the fuel jet exit velocity ranges between 31.8 m/s and 35.8 m/s ($\mathrm{Re_{Dj}} = 8200$ to 9200). An axisymmetric DBD actuator is fabricated into the outer surface of the nozzle 15 mm upstream of the nozzle exit. The exposed and embedded electrodes are 0.1 mm thick copper strips oriented perpendicular to the coflow and aredesigned to induce wall jets that oppose the coflow direction. The electrode pairs, driven by an 8 kHz, 10–12-kV peak-to-peak ac voltage, and consume 1–2 W, as determined from the driving frequency and the integrated area under the characteristic charge (Q)–applied voltage (V) curve [19]. The maximum speed of the induced wall jets, determined by particle image velocimetry (PIV), were found to be in the range 0.8–1.2 m/s. Kapton tape (200-μm thick) is used as a dielectric material to isolate the embedded electrode from the exposed electrode, which are 7 and 12-mm wide, respectively. The nozzle body has a 25° taper to reduce the propensity for coflow separation because of the nozzle body itself.

Stereo PIV (sPIV) and unfiltered chemiluminescence imaging are employed to characterize the flow velocity field with minimal error from out of plane motion and also the location of the turbulent jet diffusion flame base, as schematically shown in Fig. 1(b). A Nd:YAG laser (New wave, Gemini PIV, 100 mJ/pulse energy, 3 Hz, 532 nm) is shaped into a thin sheet using two cylindrical lenses and a convex spherical lens, and directed into the test section for the PIV studies. Two double exposure charged-coupled device (CCD) cameras (LaVision, Imager Intense) capture the scattered light from submicrometer size alumina particles that are seeded into the flow upstream of the flow-straightening honeycomb. The unfiltered flame chemiluminescence is carried out with an intensified CCD camera (Princeton Instrument, PI-MAX). A 200-ns gate width is used for the chemiluminescence imaging.

The anticipated flow structure that is induced by the DBD actuator is described qualitatively in Fig. 2(a). The actuator is expected to generate a separation bubble in the vicinity of the electrodes because the direction of the induced flow is opposite to that of the surrounding coflow. The air flow is diverted around the separation bubble and then entrained by the jet flow. Fig. 2(b) shows the various regions imaged for analysis. Imaging of the unfiltered chemiluminescence was performed over the field of view (FOV) designated as (FOV 1). PIV measurements were conducted over the regions designated as FOV 2 and 3. FOV 1 is 70 mm in length starting 5-mm downstream of the jet nozzle exit and 25-mm wide. Chemiluminescence images taken over this region have a 130-μm/pixel spatial resolution. Over 100 instantaneous images were taken to determine the location of the ethane turbulent jet diffusion flame base. A representative example of an unfiltered flame chemiluminescence image is shown in Fig. 3. The white dashed line represents the base of the flame as determined by edge detection methods in MATLAB's Image Processing Toolbox. FOV 2 is 40 mm in length starting 40-mm upstream of the jet nozzle exit and 40 mm in width from the surface of the nozzle body. FOV 3 is 40 mm in length from the jet nozzle exit and 35 mm in width starting 5 mm from the jet nozzle centerline. To obtain an ensemble averaged velocity field, 200 instantaneous image pairs with 50-μm/pixel spatial resolution separated by 200 μs between imaging frames, were taken at FOV 2 and 3. Laser shot timing and the triggering of the cameras are synchronized by a delay generator (SRS, DG 535). The images taken at FOV 2 and 3 were processed

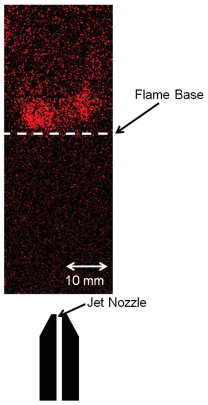

Fig. 3. Representative instantaneous image of unfiltered intensified flame chemiluminescence.

by a commercial software package, Davis 7 [LaVision GmbH]. Decreasing the interrogation size with a multipass calculation, two passes for 64-by-64 pixels and two passes for 32-by-32 pixels, with 50% overlap were selected for the vector velocity calculation.

III. Result and Discussion

The locations of the flame base for four different fuel jet exit speeds, 31.8, 33.2, 34.6, and 35.8 m/s, are measured. The mean and standard deviations of the locations relative to the jet nozzle at three different coflow speeds are plotted in Fig. 4. The tendency of these results for flows without actuation, higher liftoff height with higher coflow speed, are consistent with previous studies [20] that have provided liftoff height as a function of coflow speed. Flows without actuation, 10, 11, and 12-kV peak-to-peak voltage actuations are represented as red circles, blue squares, black crosses, and green triangles, respectively. At 0.3-m/s coflow speed, as shown in Fig. 4(a), there is no significant effect of actuation on the flame base location except perhaps at the 12-kV case. The effect of DBD actuation, however, is more significant when the speed of the coflow air increases, as shown in Fig. 4(b) and (c). The liftoff height of the turbulent jet diffusion flame decreases between 30% and 40% when compared with the height without actuation.

The tendency for there to be a greater effect of DBD actuation on flame liftoff height with increasing discharge voltage and coflow speed can be explained by comparing mean velocity fields. Fig. 5 shows the mean streamwise velocity (u_y) contours in FOV 2 normalized by the freestream speed (u_∞). The case in which there is no actuation is shown in Fig. 5(a), 10-kVp-p actuation in Fig. 5(b), 11-kVp-p actuation in Fig. 5(c), and 12-kVp-p actuation in Fig. 5(d). All cases in Fig. 5 are for a 0.3-m/s coflow speed and 34.6-m/s fuel jet speed. For reference, the length scale of the images and the location of the nozzle body are shown in Fig. 5(a). White dashed lines in these figures are lines of constant speed (0.99 u_∞) that aid in distinguishing a departure from the freestream flow conditions. It is clear that the redirected flow as a result of actuation at low discharge voltage [10-kVp-p voltage, Fig. 5(b)] recovers to nearly the free stream

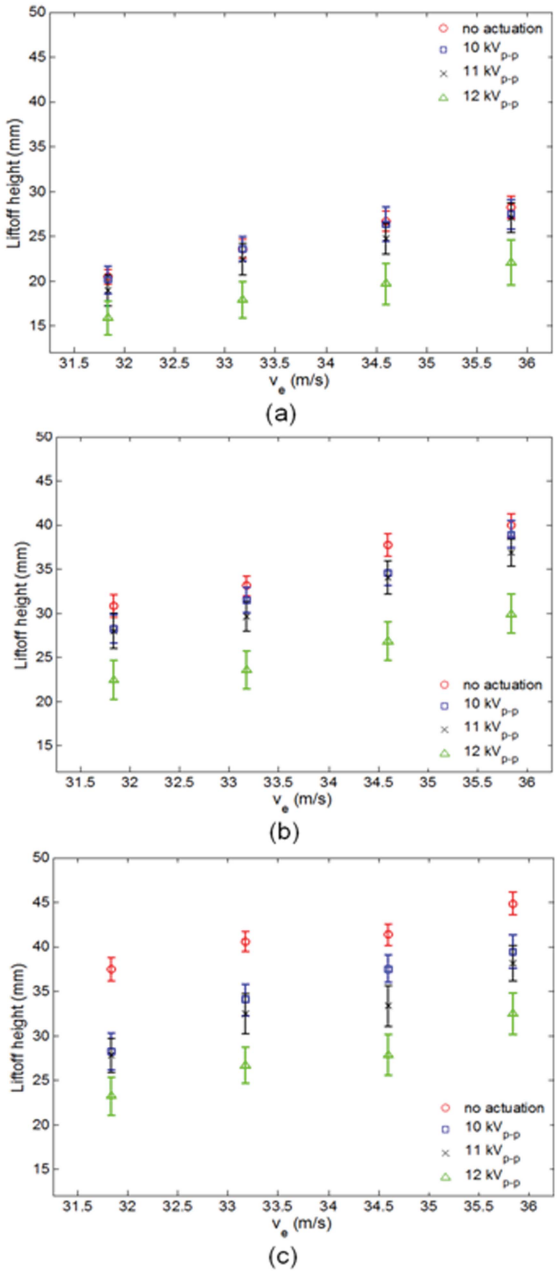

Fig. 4. Mean and standard deviation of flame base locations without actuation and with actuation for a 10–12 kV peak-to-peak voltage at (a) 0.3-, (b) 0.45-, and (c) 0.6-m/s coflow speed.

conditions at the location of the fuel jet nozzle exit. The area of the actuation-affected region increases with increasing discharge voltage [Fig. 5(c) and (d)]. The extent of this is more apparent when we compare the PIV results for the downstream mean velocity field (FOV 3), as shown in Fig. 6. Fig. 6(a) shows the mean streamwise velocity (u_y) contours in FOV 3 normalized by the freestream speed (u_∞) for no actuation. Cases for actuation at increasing discharge voltages are shown in Fig. 6(b)–(d) for the 10-, 11-, and 12-kVp-p conditions, respectively, for the same jet and coflow conditions of Fig. 5. The length scale and the location of the nozzle body are shown in Fig. 6(a). Once again, the effect of actuation on the flow is small at 10 kVp-p [Fig. 6(b)] but noticeable changes are

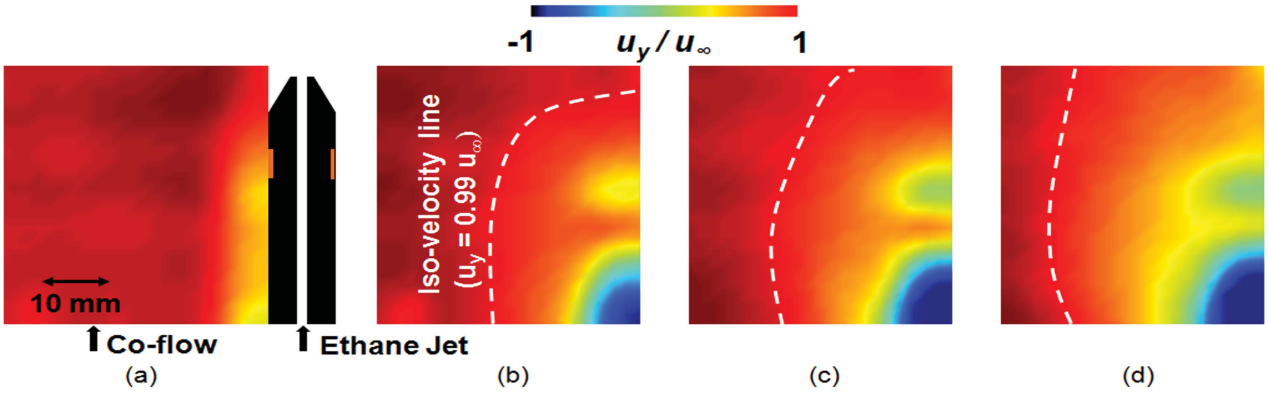

Fig. 5. Normalized mean streamwise velocity (u_y) contour of FOV 2 at 0.3-m/s coflow speed (u_∞) (a) without actuation, and (b) with 10-, (c) 11-, and (d) 12-kVp-p voltage actuation in the presence of a reacting jet with 34.6-m/s jet exit speed.

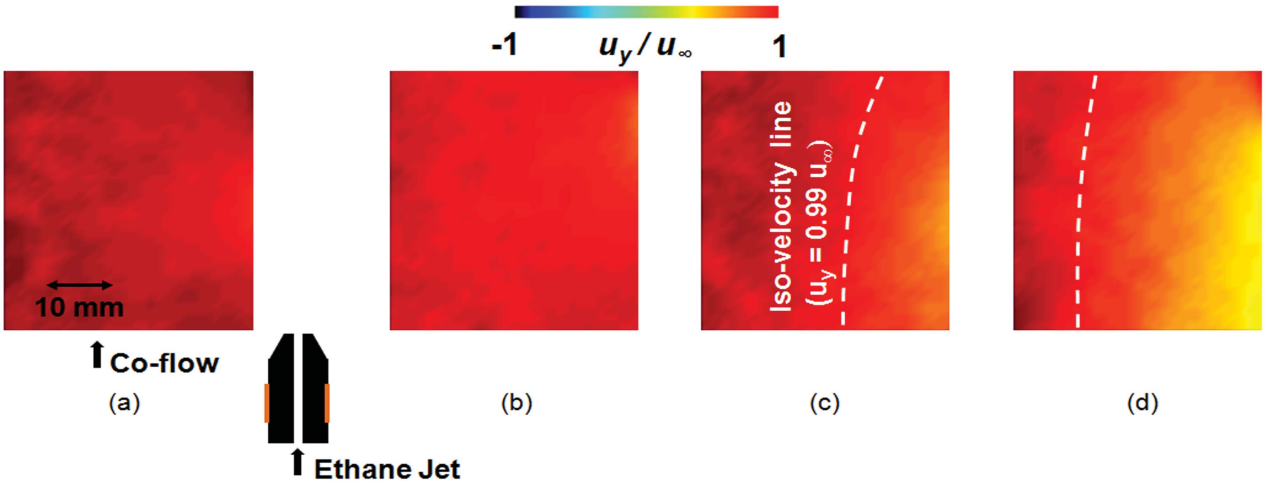

Fig. 6. Normalized mean streamwise velocity (u_y) contour of FOV 3 at 0.3-m/s coflow speed (u_∞) (a) without actuation, and with (b) 10-, (c) 11-, and (d) 12-kVp-p voltage actuation in the presence of a reacting jet with 34.6-m/s jet exit speed.

observed in FOV 3 when higher voltages are applied to the DBD actuator.

Despite the relatively significant effect that the 11-kVp-p voltage actuation has on the flow field at the 0.3-m/s coflow speed [Figs. 5(c) and 6(c)], the reduction in the distance of the flame base from the jet nozzle exit is small [Fig. 4(a)]. This was at first surprising, but it is known that the heat release from the flame can also strongly perturb the flow field [20]. It is desirable then, to separate the effect on the flow field by actuation and heat release. To do so, we carried out identical PIV studies without igniting the ethane jet. The results for this baseline study are shown in Fig. 7. Fig. 7(a) is the nonactuated flow condition, whereas Fig. 7(b) is the 10-kVp-p actuation case. The 10-kVp-p actuation does not seem to affect the flow, and although there is a small perturbation in the flow at 11 kVp-p, Fig 7(c) confirms that this case is much weaker than the combusting case. Unlike the 10 and 11-kVp-p actuation cases, there are significant changes in both the flame liftoff height and flow field as a result of 12-kVp-p actuation, as shown in Figs. 4(a) and 5–7(d).

Fig. 8 shows the mean streamwise velocity (u_y) contours in FOV 2 normalized by the freestream speed (u_∞) for the highest coflow speed case studied (0.6 m/s) and, again, with the presence of an ignited ethane jet at 34.6-m/s nozzle exit speed. The case without actuation is shown in Fig. 8(a), with 10-kVp-p actuation in Fig. 8(b), with 11-kVp-p actuation in Fig. 8(c), and with 12-kVp-p actuation in Fig. 8(d). The length scale and the location of the nozzle body are shown in Fig. 8(a). The effect of the increased coflow speed is apparent, with actuation having a much stronger perturbation on the flow at all discharge voltages when compared with the lower 0.3-m/s coflow speeds (Fig. 5). This was unexpected, as it was thought that the increased coflow speed would have a diminishing effect on the discharge coupling to the flow. We believe that this is caused by the direction of the induced flow, which opposes the incoming coflow direction. When the coflow is perturbed by the DBD actuation, it tends to recover to its initial speed at a distance downstream of the flow actuation. In higher coflow speeds, the convected length scale of the perturbed flow is much longer, i.e., the convection time scale is shorter, so the perturbed fluid reaches the flame base and modifies its position. It is apparent that the affected flow region is larger as the actuation strength increases, as shown in Figs. 5–8. Because the size of the induced separation bubble is larger with higher applied voltage, the surrounding

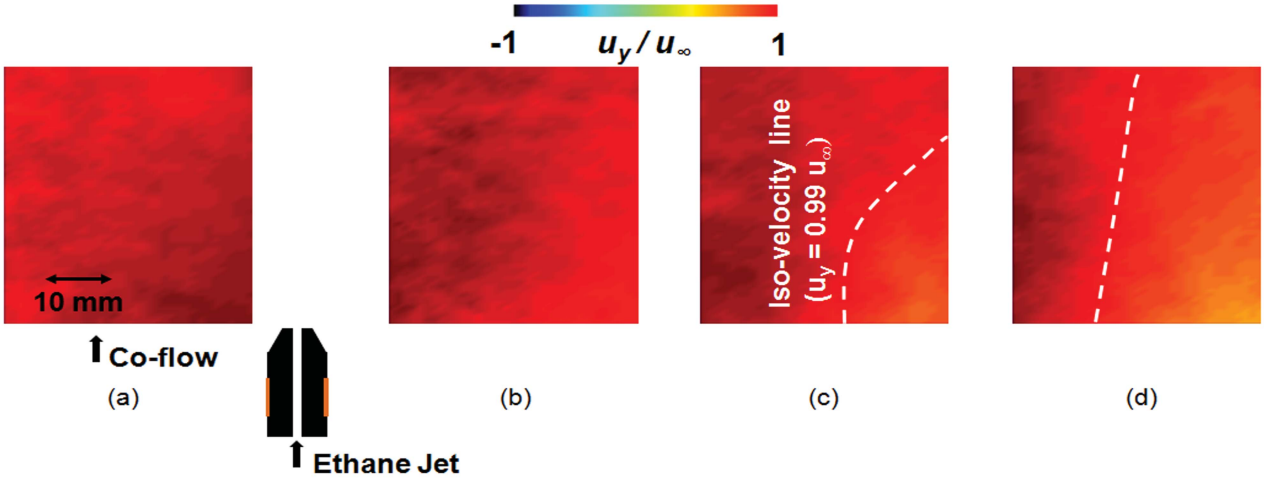

Fig. 7. Normalized mean streamwise velocity (u_y) contour of FOV 3 at 0.3-m/s coflow speed (u_∞) (a) without actuation, and with (b) 10-, (c) 11-, and (d) 12-kVp-p voltage actuation in the presence of a nonreacting jet with 34.6-m/s jet exit speed, i.e., there is no ignition.

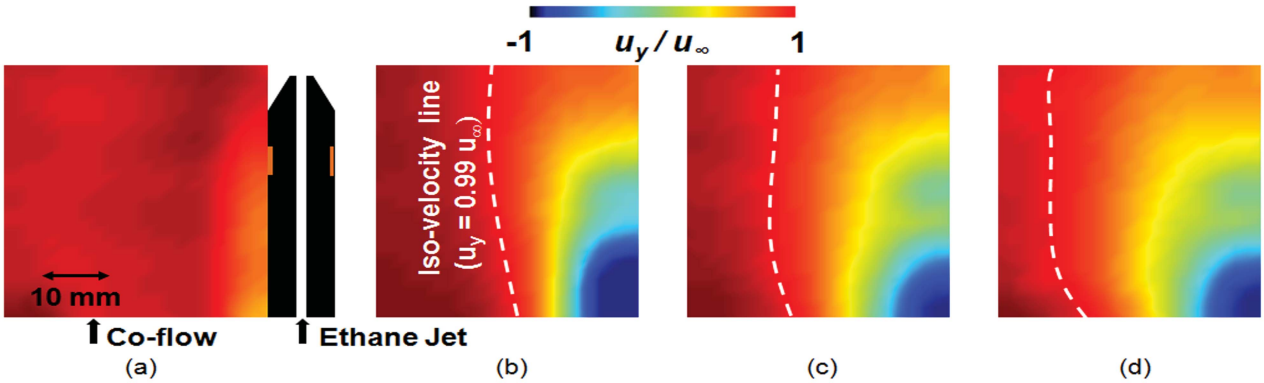

Fig. 8. Normalized mean streamwise velocity (u_y) contour of FOV 2 at 0.6-m/s coflow speed (u_∞) (a) without actuation, and with (b) 10-, (c) 11-, and (d) 12-kVp-p voltage actuation in the presence of a reacting jet with 34.6-m/s jet exit speed.

air behaves as if there is a larger bluff body present. As a result, there is a much stronger actuation effect when a higher voltage is applied to the DBD actuator, as shown in Fig. 4. It is also noteworthy to mention here that the effect of actuation on the location of the flame base is mainly because of the large scale modifications of the flow and not because of the effect that actuation may have on the enhancement of the mixing of the surrounding air with the fuel jet. We have made laser-induced break down measurements of the mixing region with and without plasma actuation (the results will be presented in a subsequent paper) and we have found that the spatial variation in the local fuel/air equivalence ratios are not strongly affected by the discharge actuation. PIV study on FOV 1 is currently underway to investigate the interaction between the flame and the actuated flow by the DBD actuator.

IV. Conclusion

DBD actuation control of the surrounding coflow air is used to stabilize an ethane turbulent jet diffusion flame. PIV and unfiltered flame chemiluminescence imaging are employed to characterize the mean flow field and the location of the flame base, respectively. The DBD-induced flow opposites the direction of coflow to generate a separation bubble and to redirect the air away from the fuel jet nozzle. As a result of this actuation, the flame liftoff height is shortened by 30%–40%. Higher coflow speeds exaggerate the effect, as the perturbed flow extends further downstream resulting in a larger actuated region. The size of perturbed flow is also larger with increased discharge power. Despite the relatively robust effects that actuation has on the large-scale flow features, the shear-layer mixing regions are not strongly affected by actuation, showing that stability is not a result of enhanced mixing.

References

[1] A. R. Masri and R. W. Bilger, "Turbulent diffusion flames of hydrocarbon fuels stabilized on a bluff body," in *Proc. 20th Symp. Int. Combustion*, 1984, pp. 319–326.

[2] S. M. Correa and A. Gulati, "Measurements and modeling of a bluff body stabilized flame," *Combustion Flame*, vol. 89, pp. 195–213, May 1992.

[3] Y. Chen, C. Chang, K. Pan, and J. Yang, "Flame lift-off and stabilization mechanisms of nonpremixed jet flames on a bluff-body burner," *Combustion Flame*, vol. 115, nos. 1–2, pp. 51–65, Oct. 1998.

[4] I. Esquiva-Dano, H. T. Nguyen, and D. Escudie, "Influence of a bluff-body's shape on the stabilization regime of non-premixed flames," *Combustion Flame*, vol. 127, no. 4, pp. 2167–2180, Dec. 2001.

[5] N. K. Rizk and A. H. Lefebvre, "The relationship between flame stability and drag of bluff-body flameholders," *J. Propulation Power*, vol. 2, no. 4, pp. 361–365, Jul. 1984.

[6] E. Moreau, "Airflow control by non-thermal plasma actuators," *J. Phys. D, Appl. Phys.*, vol. 40, no. 3, pp. 605–636, Feb. 2007.

[7] W. Kim, H. Do, M. G. Mungal, and M. A. Cappelli, "On the role of oxygen in dielectric barrier discharge actuation of aerodynamic flows," *Appl. Phys. Lett.*, vol. 91, no. 18, pp. 181501-1–181501-3, Oct. 2007.

[8] H. Do, W. Kim, M. A. Cappelli, and M. G. Mungal, "Cross-talk in multiple dielectric barrier discharge actuators," *Appl. Phys. Lett.*, vol. 92, no. 7, pp. 071504-1–071504-3, Feb. 2008.
[9] J. R. Roth, D. M. Sherman, and S. P. Wilkinson, "Boundary layer flow control with a one atmosphere uniform glow discharge surface plasma," in *Proc. 36th AIAA Sci. Meeting Exhibit*, Jan. 1998.
[10] C. A. Borghi, M. R. Carraro, and A. Cristofolini, "Plasma and flow characterization in a flat panel one atmosphere uniform barrier discharge," in *Proc. 36th AIAA Plasmadyn. Lasers Conf.*, Jun. 2005.
[11] H. Do, W. Kim, M. G. Mungal, and M. A. Cappelli, "Bluff body flow separation control using surface dielectric barrier discharges," in *Proc. 45th AIAA Aerosp. Sci. Meetings Exhibit*, Jan. 2007.
[12] Y. Sung, W. Kim, M. G. Mungal, and M. A. Cappelli, "Aerodynamic modification of flow over bluff objects by plasma actuation," *Exp. Fluids*, vol. 41, no. 3, pp. 479–486, Sep. 2006.
[13] S. Im, H. Do, and M. A. Cappelli, "Dielectric barrier discharge control of a turbulent boundary layer in a supersonic flow," *Appl. Phys. Lett.*, vol. 97, no. 4, pp. 041503-1–041503-3, Jul. 2010.
[14] S. Im, H. Do, and M. A. Cappelli, "The manipulation of an unstarting supersonic flow by plasma actuator," *J. Phys. D, Appl. Phys.*, vol. 45, no. 48, pp. 485202-1–485202-8, Dec. 2012.
[15] D. M. Schatzman and F. O. Thomas, "Turbulent boundary-layer separation control with single dielectric barrier discharge plasma actuators," *AIAA J.*, vol. 48, no. 8, pp. 1620–1634, Aug. 2010.
[16] K.-S. Choi, T. N. Jukes, and R. Whalley, "Turbulent boundary-layer control with plasma actuators," *Philosophical Trans. R. Soc. A*, vol. 369, no. 1940, pp. 1443–1458, Mar. 2011.
[17] T. N. Jukes and K.-S. Choi, "Dielectric-barrier-discharge vortex generators: Characterisation and optimisation for flow separation control," *Exp. Fluids*, vol. 52, no. 2, pp. 329–345, Feb. 2012.
[18] S. Im and M. A. Cappelli, "Dielectric barrier discharge induced boundary layer suction," *Appl. Phys. Lett.*, vol. 100, no. 26, pp. 264103-1–264103-4, Jun. 2012.
[19] T. C. Manley, "The electric characteristics of the ozonator discharge," *J. Electrochem. Soc.*, vol. 84, no. 1, pp. 83–96, Jul. 1943.
[20] L. Muñiz and M. G. Mungal, "Instantaneous flame-stabilization velocities in lifted-jet diffusion flames," *Combustion Flame*, vol. 111, nos. 1–2, pp. 16–31, Oct. 1997.

Seong-kyun Im received the B.S. degree in mechanical and aerospace engineering from Seoul National University, Seoul, Korea, in 2007, and the M.S. and Ph.D. degrees in mechanical engineering from Stanford University, Stanford, CA, USA, in 2009 and 2013, respectively.

He is currently a Post-Doctoral Researcher with the Stanford Plasma Physics Laboratory, Department of Mechanical Engineering, Stanford University. His current research interests include control of subsonic and supersonic aerodynamic flows, compressible flows, plasma-assisted combustion, and supersonic combustion.

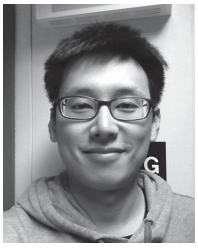

Moon Soo Bak received the B.S. degree in mechanical and aerospace engineering from Seoul National University, Seoul, Korea, in 2007, and the M.S. degree in mechanical engineering from Stanford University, Stanford, CA, USA, in 2010, where he is currently pursuing the Ph.D. degree with the Department of Mechanical Engineering.

His current research interests include combustion, fluid dynamics, plasmas, plasma-assisted combustion, and atmospheric pressure plasmas.

Mr. Bak is a recipient of the Stanford Graduate Fellowship.

Mark Godfrey Mungal was born in Trinidad, West Indies. He received the B.A.Sc. (Hons.) degree in engineering science from the University of Toronto, Toronto, ON, Canada, in 1975, and the M.S. and Ph.D. degrees in aeronautics from the California Institute of Technology, Pasadena, CA, USA, in 1977 and 1983, respectively.

He is currently the Dean of the School of Engineering, Santa Clara University, Santa Clara, CA, USA, and a Professor Emeritus with the Department of Mechanical Engineering, Stanford University, Stanford, CA, USA.

Dr. Mungal is a fellow of the American Physical Society and the American Society of Mechanical Engineers, an Associate Fellow of the American Institute of Aeronautics and Astronautics, and a member of the American Society of Engineering Education and the Combustion Institute.

Mark A. Cappelli received the B.A.Sc. degree in physics from McGill University, Montreal, QC, Canada, in 1980, and the M.A.Sc. and Ph.D. degrees in aerospace science and engineering from the University of Toronto, Toronto, ON, in 1983 and 1987, respectively.

He is currently a Professor with the Department of Mechanical Engineering, Stanford University, Stanford, CA, USA. His current research interests include plasmas and gas discharges, including plasma diagnostics, as they apply to aerodynamic and space propulsion, combustion, material processing, fusion, natural phenomenon, and medicine.